

---

This is an electronic reprint of the original article.  
This reprint may differ from the original in pagination and typographic detail.

Shah, M. A.K.Yousaf; Tayyab, Zuhra; Rauf, Sajid; Yousaf, Muhammad; Mushtaq, Naveed; Imran, Muhammad Ali; Lund, Peter D.; Asghar, Muhammad Imran; Zhu, Bin

**Interface engineering of bi-layer semiconductor  $\text{SrCoSnO}_{3-\delta}$ - $\text{CeO}_{2-\delta}$  heterojunction electrolyte for boosting the electrochemical performance of low-temperature ceramic fuel cell**

*Published in:*  
International Journal of Hydrogen Energy

*DOI:*  
[10.1016/j.ijhydene.2021.07.204](https://doi.org/10.1016/j.ijhydene.2021.07.204)

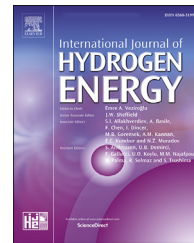
Published: 01/10/2021

*Document Version*  
Publisher's PDF, also known as Version of record

*Published under the following license:*  
CC BY

*Please cite the original version:*

Shah, M. A. K. Y., Tayyab, Z., Rauf, S., Yousaf, M., Mushtaq, N., Imran, M. A., Lund, P. D., Asghar, M. I., & Zhu, B. (2021). Interface engineering of bi-layer semiconductor  $\text{SrCoSnO}_{3-\delta}$ - $\text{CeO}_{2-\delta}$  heterojunction electrolyte for boosting the electrochemical performance of low-temperature ceramic fuel cell. *International Journal of Hydrogen Energy*, 46(68), 33969-33977. <https://doi.org/10.1016/j.ijhydene.2021.07.204>

Available online at [www.sciencedirect.com](http://www.sciencedirect.com)**ScienceDirect**journal homepage: [www.elsevier.com/locate/he](http://www.elsevier.com/locate/he)

# Interface engineering of bi-layer semiconductor SrCoSnO<sub>3-δ</sub>-CeO<sub>2-δ</sub> heterojunction electrolyte for boosting the electrochemical performance of low-temperature ceramic fuel cell

M.A.K. Yousaf Shah <sup>a,\*\*\*,1</sup>, Zuhra Tayyab <sup>b,1</sup>, Sajid Rauf <sup>b</sup>, Muhammad Yousaf <sup>a</sup>, Naveed Mushtaq <sup>a</sup>, Muhammad Ali Imran <sup>d</sup>, Peter D. Lund <sup>c</sup>, Muhammad Asghar <sup>b,c,\*</sup>, Bin Zhu <sup>a,\*\*\*</sup>

<sup>a</sup> Jiangsu Provincial Key Laboratory of Solar Energy Science and Technology/Energy Storage Joint Research Center, School of Energy and Environment, Southeast University, No. 2 Si Pai Lou, Nanjing 210096, China

<sup>b</sup> Hubei Collaborative Innovation Center for Advanced Organic Chemical Materials, Faculty of Physics and Electronic Science, Hubei University, Wuhan, Hubei, 430062, China

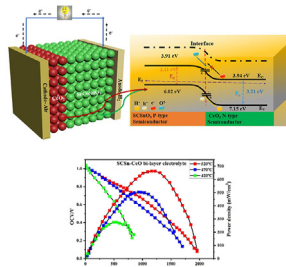
<sup>c</sup> New Energy Technologies Group, Department of Applied Physics, Aalto University School of Science, P. O. Box 15100, FI-00076 Aalto, Espoo, Finland

<sup>d</sup> Department of Agribusiness and Applied Economics MNS-University of Agriculture, Multan, Pakistan

## HIGHLIGHTS

- SrCoSnO<sub>3-δ</sub>-CeO<sub>2-δ</sub> semiconductor materials have been applied as a bi-layer electrolyte for CFC.
- The bi-layer electrolyte has a remarkable ionic conductivity of 0.2 S/cm.
- The fuel cell device produced 672 mW/cm<sup>2</sup> at 520 °C.
- Bi-layer electrolyte was studied via band alignment mechanism based on proposed p-n heterojunction.

## GRAPHICAL ABSTRACT



## ARTICLE INFO

### Article history:

Received 19 January 2021

Received in revised form

21 July 2021

## ABSTRACT

A comparative study is performed to investigate the electrochemical performance of the low-temperature ceramic fuel cells (CFCs) utilizing two different novel electrolytes. First, a perovskite semiconductor SrCo<sub>0.3</sub>Sn<sub>0.7</sub>O<sub>3-δ</sub> was used as an electrolyte in CFCs due to its modest ionic conductivity (0.1 S/cm) and demonstrated an acceptable power density of 360 mW/cm<sup>2</sup> at 520 °C. The performance of the cell was primarily limited due to the

\* Corresponding author. Hubei Collaborative Innovation Center for Advanced Organic Chemical Materials, Faculty of Physics and Electronic Science, Hubei University, Wuhan, Hubei, 430062, China.

\*\* Corresponding author.

\*\*\* Corresponding author.

E-mail addresses: [alikamranshah91@gmail.com](mailto:alikamranshah91@gmail.com) (M.A.K.Y. Shah), [imran.asghar@aalto.fi](mailto:imran.asghar@aalto.fi) (M.I. Asghar), [binzhu@kth.se](mailto:binzhu@kth.se) (B. Zhu).

<sup>1</sup> These two authors contributed equally.

<https://doi.org/10.1016/j.ijhydene.2021.07.204>

Accepted 27 July 2021  
Available online 18 August 2021

**Keywords:**

Ceramic fuel cell  
Bi-layer electrolyte  
Semiconductor heterojunction  
Built-in electric field

moderate ionic transport in the electrolyte. In order to improve the ionic conductivity, a new strategy of using a novel bi-layer electrolyte concept consist of  $\text{SrCo}_{0.3}\text{Sn}_{0.7}\text{O}_{3-\delta}$  and  $\text{CeO}_{2-\delta}$  in CFCs. These bi-layers of two electrolytes have successfully established heterojunction which considerably improved the ionic conductivity (0.2 S/cm) and enhance the open-circuit voltage of the cell from 0.98 V to 1.001 V. Moreover, the CFCs utilizing bi-layer electrolyte have produced a remarkable power density of  $672 \text{ mW/cm}^2$  at  $520^\circ\text{C}$ . This enhancement of ionic conduction, power density and blockage of electron conduction in the bi-layer electrolyte was studied via band alignment mechanism based on proposed p-n heterojunction. Our work presents a promising methodology for developing advanced low-temperature CFC electrolytes.

© 2021 The Author(s). Published by Elsevier Ltd on behalf of Hydrogen Energy Publications LLC. This is an open access article under the CC BY license (<http://creativecommons.org/licenses/by/4.0/>).

## Introduction

Achieving high ionic conduction at low temperatures is the key research challenge in the development of advanced semiconductor-based ceramic fuel cells (SCFCs). One way to improve the performance of SCFCs is to utilize a mix of  $\text{O}^{2-}$  and  $\text{H}^+$  conducting ceramic electrolyte materials. Generally, oxygen vacancies can be created in the solid oxide materials via doping through one or more dopants, where the created oxygen vacancies help in the transportation of  $\text{O}^{2-}$  ions which leads to improve the ionic conductivity. For instance, it is well established that the doping of Y into the  $\text{ZrO}_2$  improves its ionic conductivity and sustains the stability of YSZ material; also, Er doping into the  $\text{BiO}_3$  aids not only in stabilizing the  $\delta$ -phase structure but also helps in creation of O-vacancies (oxygen-vacancies) [1–3]. Furthermore, various reports are published where the ionic conduction was enhanced via appropriate doping such as doped ceria and Sr–Mg co-doped  $\text{LaGaO}_3$  (LSGM) [4,5]. However, the ceria-based electrolytes are constrained due to their instability and inhibiting of electronic leakage due to ease reduction of  $\text{Ce}^{+4}$  to  $\text{Ce}^{+3}$ . Usually, this happens when they are being exposed to the reducing environments.

On the other hand, extensive efforts have been made on developing the new electrodes with mixed electronic and ionic conductivities (MIEC) such as  $\text{LaSrCoFeO}_{3-\delta}$  (LSCF),  $\text{LaSrCoO}_3$  (LSCO),  $\text{BaSrCoFeO}_{3-\delta}$  (BSCF). Also, the layered structure  $\text{LaBaCo}_2\text{O}_{5+\delta}$  (LBCO), which can extend the oxygen reduction reaction (ORR) active zone to the entire surface because these can support both excellent ionic and electronic conduction [6–13]. The MIEC materials allow the redox reactions to occur on their surface and hence increase the concentration of reaction sites as well as enhance the triple-phase boundary (TPB). Therefore, MIEC materials can play a crucial role in reducing the operating temperature  $<600^\circ\text{C}$  of the CFCs [14–16]. Considering the above-mentioned features in recent years the layer structured NCAL ( $\text{LiNi}_{0.8}\text{Co}_{0.15}\text{Al}_{0.05}\text{O}_2$ ) electrodes have been reported due to its higher ORR and HOR catalytic activity [17–20].

Lately, researchers have been exploring the interfacial engineering between the semiconductor and ionic conductor to enhance the ionic conductivity of the ceramic electrolyte. Several combinations of semiconductors and ion-conducting

materials have been reported where they have reported enhancement in ionic conductivity as a result of interfacial engineering, such as YSZ/SrTiO<sub>3</sub>, SFT/SDC, and CoFe<sub>2</sub>O<sub>4</sub>/GDC [21–24]. The main idea is that these heterostructure materials are quite different and much flexible than those single-phase materials. At the interface, the electrons of the acceptor molecular state shifted to the donor state. This transformation of electrons causes to decrease in the density of surface states. Therefore, the heterostructure phase of semiconductor provides an alternative route to ionic transport, which boosts the ionic conductivity [25]. As mentioned earlier and already reported previously that semiconductor heterostructure is beneficial for high ionic conduction. In detail study, it should keep in view that p-n heterojunction has been proposed based on nano-redox reactions and nano fuel cells. The primary function of p-n heterojunction is to hinder the recombination of electron and hole pairs by developing the built-in potential [26–28]. Recently, the p-n heterojunction has been followed using  $\text{Na}_2\text{CO}_3$  (p-type) composited with  $\text{CeO}_2$  (n-type) and has successfully delivered peak power density 1 W at quite low temperature  $520^\circ\text{C}$ . Build in electric field (BIEF) induced metallic states have caused to enable the enhanced proton transport via using p-n heterostructure [29]. Also, it has been recognized that the semiconductor-ionic conductor is a well-known model to realize the ionic conductivity even at low temperature ( $450$ – $550^\circ\text{C}$ ) [30,31]. Moreover, the energy bands play the main character in affecting ionic transport in the semiconductor.

Interestingly, un-doped or pure ceria has been used as an electrolyte in SOFC operating at low temperatures [32,33]. Also, Ceria and doped ceria has been used as a single phase as well as a composite semiconductor heterostructure electrolyte, which has delivered a better performance as well as high ionic conductivity [5,32,33]. Besides, lately new semiconductor-based electrolyte either single-phase or heterostructure have reported appreciable performance along with high ionic conductivity [34–37].

Following the ideas mentioned above, herein we investigated the effect of bi-layer semiconductor heterojunction electrolyte on the electrochemical performance of SCFCs. The formation of heterojunction  $\text{SrCo}_{0.3}\text{Sn}_{0.7}\text{O}_{3-\delta}$ – $\text{CeO}_2$  causes to enhance the ionic conductivity from 0.11 to 0.2 S/cm of the individual component electrolyte. The cells utilizing this

heterojunction electrolyte produced a remarkable power density at quite low-temperature 520 °C. Moreover, more importantly, the interface of the constructed heterojunction hinders the short-circuiting of the cell. Therefore, special attention has been paid at the construction of  $\text{SrCo}_{0.3}\text{Sn}_{0.7}\text{O}_{3-\delta}$ - $\text{CeO}_2$  heterojunction at the interface and their effect on the performance of the fuel cells. This approach may enable low-temperature operation of the high-performance SCFCs and hence facilitates their commercialization.

## Experimental section

The Sol-gel technique was used to prepare the semiconductor  $\text{SrCo}_{0.3}\text{Sn}_{0.7}\text{O}_{3-\delta}$  perovskite electrolyte. A detailed description of the synthesis is mentioned here. The nitrates of Sr, Co, and Sn (99% purity sigma Aldrich) were dissolved in water with a ratio of 1:2 with citric acid and then heated the precursor solution at 80 °C with gentle stirring for 8 h to obtain the delicate brown gel of  $\text{SrCo}_{0.3}\text{Sn}_{0.7}\text{O}_{3-\delta}$  electrolyte. The purpose of adding the citric acid ( $\text{C}_6\text{H}_8\text{O}_7\text{H}_2\text{O}$ ) to the above solution as a chelating agent to prevent it from the formation of larger crystals and the aggregates of the particles. After the formation of gel,  $\text{SrCo}_{0.3}\text{Sn}_{0.7}\text{O}_{3-\delta}$  was heated at 120° for the whole night to obtain the dried powder, then ground to crush the powders homogeneously. Subsequently, the powders were sintered at 1100 °C for 8 h to obtain final electrolyte powder. Besides, ceria was synthesized using the same technique sol-gel by pouring nitrate of ceria (99.9% purity, Sigma Aldrich) into distilled water separately stirred at 80 °C for 6 h to gain elegant sol of ceria. Also, ceria powder was prepared independently for further characterization detailed given elsewhere [32].

The electrolyte powder was characterized via different characterizing tools such as the phase was studied of the  $\text{SrCo}_{0.3}\text{Sn}_{0.7}\text{O}_{3-\delta}$  and  $\text{CeO}_2$  via X-ray diffraction (XRD). The Bruker D-8 x-ray diffractometer (XRD, Bruker Corporation, Germany) operating at 45 kV and 40 mA voltage and current, respectively, with radiation of Cu K-alpha ( $\lambda = 1.54060 \text{ \AA}$ ) was used. The morphology and cross-sectional views of powder and cell were investigated by field emission scanning electron microscopy (FE-SEM, japan) working at 15 kV. To study the band alignment, UV-visible spectroscopy was used to determine the optical bandgap which operated on a UV3600 spectrometer (MIOSTECHPTY Ltd.). Moreover, Ultra photoelectron spectroscopy (UPS) was performed to investigate the position of the valence band.

The NCAL powder for use as an electrode was bought from China, Tianjin Bamo & Technology joint-stock Ltd. Besides, the Ni-foam was applied as a current collector and for cell support. Also, Terpinol was used as a binder in the fabrication of electrodes or electrolyte. Later NCAL powder was mixed with a binder (Terpinol) to get the slurry. Then slurry was applied on Ni foam of 13 mm diameter subsequently heated it at 120 °C for 20 min to dry the electrodes. To prepare the pellet at first electrolytes containing the  $\text{SrCoSnO}_{3-\delta}$  layer was pressed with 250 MPa of 13 mm diameter to obtain the pellet. Afterward, the Ceria layer coated on a single layer of  $\text{SrCoSnO}_{3-\delta}$  electrolyte material using a brush coating technique to gain final bi-layer electrolyte materials.

Then cells were sintered at 700 °C for 6 h to make the cell denser. After sintering, the bi-layer electrolyte was sandwiched between two NCAL electrodes and compressed under the pressure of 250 MPa to obtain the pellet of 13 mm diameter. The active area of the prepared pellet Ni-NCAL/ $\text{SrCoSnO}_{3-\delta}$ - $\text{CeO}_2$ /NCAL-Ni was  $0.64 \text{ cm}^2$ . The thickness of whole pellet was about 1.5 mm where's the thickness of single layer electrolyte was 700  $\mu\text{m}$ . Also, the thickness of bi-layer electrolyte (310  $\mu\text{m}$  & 400  $\mu\text{m}$ ) concerned to the  $\text{CeO}_2$  and  $\text{SrCoSnO}_3$  electrolyte layer respectively. The electrochemical performance was operated under the hydrogen fuel and ambient air with a flow rate of 150 ml  $\text{min}^{-1}$ . The impedance analysis was measured by using the electrochemical workstation (Gamry Reference 3000, USA) in the frequency range of 0.1 Hz–1 MHz with an amplitude of 10 mV. The cell performance I–V & I–P reading were obtained using electronic load (IT8511, ITEC Electrical Co., Ltd).

## Results and discussion

### X-ray diffraction (XRD)

The obtained X-ray diffraction patterns of  $\text{SrCo}_{0.3}\text{Sn}_{0.7}\text{O}_{3-\delta}$  and transparent ceria have been illustrated in Fig. 1. The peaks of the  $\text{SrCo}_{0.3}\text{Sn}_{0.7}\text{O}_{3-\delta}$  semiconductor can be indexed as a cubic perovskite structure without showing any impurities peaks. All sharped peaks revealed a well-developed crystalline structure. In addition, the characteristics peaks of the synthesized  $\text{CeO}_2$  powder at 800 °C, corresponds to the pure fluorite perovskite structure with no trace of impurities. Following the Scherrer formula, the calculated crystalline size of 48, and 50 nm corresponds to the  $\text{SrCo}_{0.3}\text{Sn}_{0.7}\text{O}_{3-\delta}$  and pure ceria, respectively. All the extracted peaks from the diffractogram are related to the individual ceria and  $\text{SrCo}_{0.3}\text{Sn}_{0.7}\text{O}_{3-\delta}$ . All peaks including (200), (220), (400), (420), (422), (440), and (620), and (111), (200), (220), (311), (222), (400), (331) and (420), are assigned to  $\text{SrCo}_{0.3}\text{Sn}_{0.7}\text{O}_{3-\delta}$  (JCPD no. 00-042-1467) and  $\text{CeO}_2$  (JCPD no. 43-1002) respectively. Also, diffraction pattern of  $\text{SrCo}_{0.3}\text{Sn}_{0.7}\text{O}_{3-\delta}$  displays minors peaks at 26- and 34-degrees corresponds to the  $\text{SrCO}_3$ . Moreover, the peaks well-matched with the reported literature [33,38,39]. Moreover, lattice volume from XRD and Archimedes principle unveiled the relative density of sintered pellets for SCSn– $\text{CeO}_2$  is 93% while 87% for the single layer SCSn electrolyte suggesting that bi-layer electrolyte is much denser than the single layer.

### Scanning electron microscopy (SEM)

Fig. 2 (a) shows the ceria electrolyte layer between the cathode and  $\text{SrCo}_{0.3}\text{Sn}_{0.7}\text{O}_{3-\delta}$  electrolyte layer, and Fig (b) exhibits a magnified image of the three layers of the fuel cell. These depicted images confirm that the ceria has been well incorporated as a bi-layer with the  $\text{SrCo}_{0.3}\text{Sn}_{0.7}\text{O}_{3-\delta}$  electrolyte as well as with the electrode, which is helpful for the fuel cell performance. Fig (c) magnified the surface of the ceria electrolyte layer.

Fig. 2(d) shows the cross-sectional view of single layer fuel cell device. It can be clearly noticed that electrolyte is dense and sandwiched between the porous electrode which guarantee

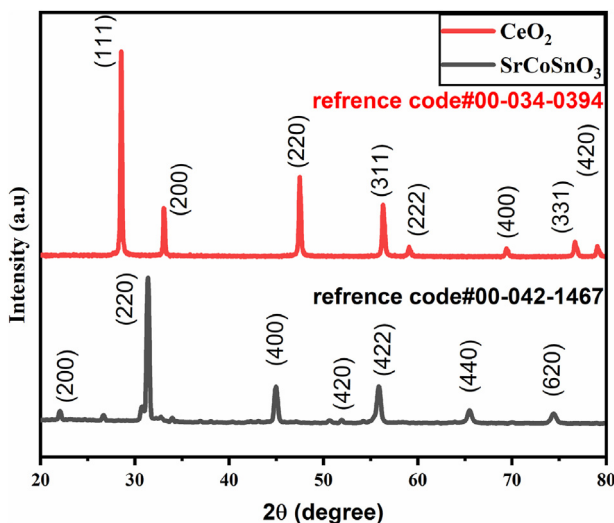


**Fig. 1 – X-ray diffraction pattern of  $\text{SrCo}_{0.3}\text{Sn}_{0.7}\text{O}_{3-\delta}$  and  $\text{CeO}_2$ .**

better current density, higher OCV and high catalytic activity of electrode. While Fig. 2(e–f) visualized the images of the scanning electron microscopy (SEM) of the ceria and  $\text{SrCoSnO}_{3-\delta}$  powder, which reveals that the particles are uniformly distributed. From the morphological aspects, it has shown that particle size does matter in case of grain and has a strong correlation with the flow of charge carriers. The uniformity of the current materials revealed that particles (grains) are well connected, which is beneficial for the transportation of charges. The small size of grains discloses the fast transport of charges and also decreased grain boundary (GB) to produce more active area sites directly. The homogeneity of all particles is in favor of quick transport of charge carrier in our device. Consequently, the interface in the heterostructure is much more suitable area to speed-up the charge transport in our device.

### Fuel cell performance

To demonstrate the electrochemical performance, the current-voltage ( $I-V$ ) and current-power ( $I-P$ ) curves of the symmetrical solid oxide fuel cells, ( $\text{Ni-NCAL/SrCo}_{0.3}\text{Sn}_{0.7}\text{O}_{3-\delta}/\text{NCAL-Ni}$ ) and ( $\text{Ni-NCAL/SrCo}_{0.3}\text{Sn}_{0.7}\text{O}_{3-\delta}-\text{CeO}_{2-\delta}/\text{NCAL-Ni}$ ), are shown in Fig. 3. All these measurements were carried out under different gas environments (hydrogen as a fuel and air as an ambient oxidant), as presented in Fig. 3 (a, b). The cells involve  $\text{SrCo}_{0.3}\text{Sn}_{0.7}\text{O}_{3-\delta}$  and  $\text{SrCo}_{0.3}\text{Sn}_{0.7}\text{O}_{3-\delta}-\text{CeO}_{2-\delta}$  as electrolytes have generated a remarkable high-power density of 80, 290 and 360  $\text{mW/cm}^2$  and 250, 510 and 672  $\text{mW/cm}^2$  at 420 °C, 470 °C and 520 °C, respectively.

The cell utilizing pure  $\text{SrCo}_{0.3}\text{Sn}_{0.7}\text{O}_{3-\delta}$  has less open-circuit voltage (OCV) than 1.0 V, which suggests that there is some gas leakage or short circuit issue. However, in the fuel cell involve  $\text{SrCoSnO}_{3-\delta}-\text{CeO}_{2-\delta}$  has stable and more than 1.0 V OCV with higher performance 672  $\text{mW/cm}^2$ , which manifests that the heterojunction is suitable for fuel cell technology, as reported in previous reports [21,40,41]. Such high performance has two reasons; (i) one of them is the incorporation of the pure ionic conductor into the  $\text{SrCo}_{0.3}\text{Sn}_{0.7}\text{O}_{3-\delta}$  mix conductor in the form of the bilayer electrolyte (ii) second is the formation of heterojunction which overall enhances the ionic conduction and stop the electronic conduction, such high ionic conduction contributed from the interface of  $\text{SrCo}_{0.3}\text{Sn}_{0.7}\text{O}_{3-\delta}-\text{CeO}_{2-\delta}$  leads to higher performance as reported in many cases [23]. Generally, it is established that in the fuel cell science, e-conduction (electronic conduction) is not suitable for an electrolyte, but in some extent the e-conduction help our proposed concept of bi-layers electrolyte. The e-conduction not only has a negative consequence but also has a positive impact on a fuel cell as it helps to enhance the TPB region of cathode and anode, which causes decay in polarization resistance [42]. In contrast, the dominance of e-conduction can cause a short-circuiting problem, which has not been observed in  $\text{SrCo}_{0.3}\text{Sn}_{0.7}\text{O}_{3-\delta}-\text{CeO}_2$  heterostructure.

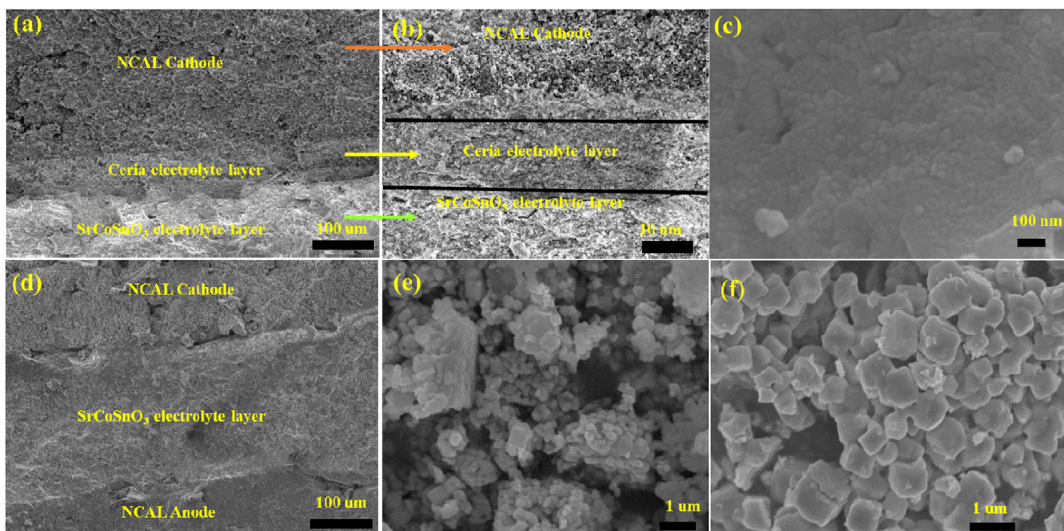


**Fig. 2 – Micrograph of (a–b) the cross-sectional view of bi-layer electrolyte and, electrolyte pasted cathode supported layer of ceria with different resolution (c) the surface of the ceria electrolyte layer, (d) the cross-sectional view of single layer electrolyte ( $\text{Ni/NCAL-SCSn-NCAL/Ni}$ ) and (e–f) the images of Ceria and  $\text{SrCoSnO}_{3-\delta}$  powder.**

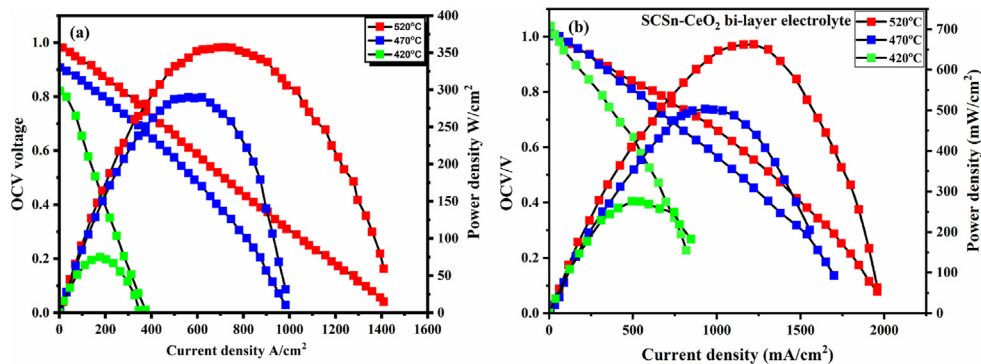


**Fig. 3 – I–V/I–P curve of (a)  $\text{SrCo}_{0.3}\text{Sn}_{0.7}\text{O}_{3-\delta}$  and (b)  $\text{SrCo}_{0.3}\text{Sn}_{0.7}\text{O}_{3-\delta}$  - $\text{CeO}_2$  bi-layer electrolyte operated at different temperature 450–550 °C.**

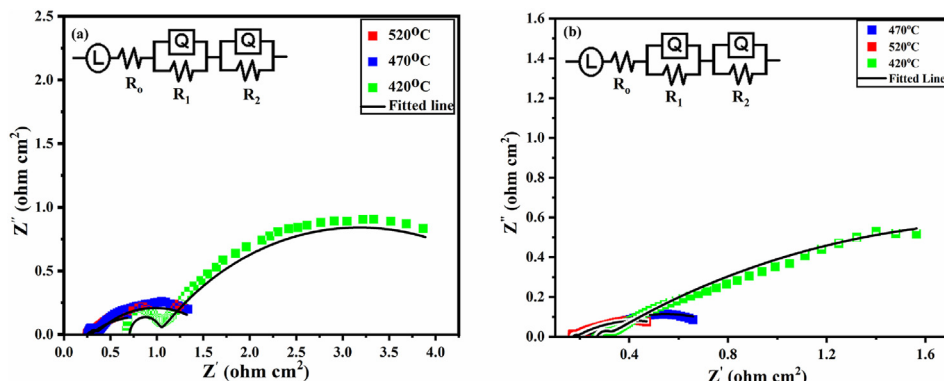


**Fig. 4 – Electrochemical Impedance Spectroscopy of (a)  $\text{SrCo}_{0.3}\text{Sn}_{0.7}\text{O}_{3-\delta}$  and (b)  $\text{SrCo}_{0.3}\text{Sn}_{0.7}\text{O}_{3-\delta}$  - $\text{CeO}_2$  bi-layer electrolyte at different temperature 420–520 °C.**

Following the fuel cell performance, the EIS characterization was carried out to investigate the electrochemical properties of the two of cells (Ni-NCAL/ $\text{SrCo}_{0.3}\text{Sn}_{0.7}\text{O}_{3-\delta}$ -NCAL-Ni and Ni-NCAL/ $\text{SrCo}_{0.3}\text{Sn}_{0.7}\text{O}_{3-\delta}$  - $\text{CeO}_2$ /NCAL-Ni). Fig. 4 (a, b) shows the impedance spectra of the single-layer  $\text{SrCo}_{0.3}\text{Sn}_{0.7}\text{O}_{3-\delta}$  and  $\text{SrCo}_{0.3}\text{Sn}_{0.7}\text{O}_{3-\delta}$  - $\text{CeO}_2$  heterostructure layer operated under the OCV condition at 420–520 °C. Normally, the intercept at high frequency at the real axis manifests the ohmic resistance ( $R_o$ ) and the ohmic resistance ( $R_o$ ) contained the resistance of the electrolyte and electrodes, and the ohmic contact resistance that usually comes from the interface [41]. In addition, to the ohmic resistance, the polarization resistance  $R_p$  which is the sum of  $R_1$  and  $R_2$  corresponds to charge transfer and mass transfer at high frequency (HF) and low frequency (LF). Polarization resistance ( $R_p$ ) constitutes several despondent arcs signifying the existence of physical as well as the chemical process corresponds to the anode and cathode as briefed earlier [5].

The obtained ohmic resistance ( $R_o$ ) of the cells are about  $0.18 \Omega\text{-cm}^2$ , and  $0.25 \Omega\text{-cm}^2$  corresponding to the  $\text{SrCo}_{0.3}\text{Sn}_{0.7}\text{O}_{3-\delta}$  - $\text{CeO}_2$  and  $\text{SrCo}_{0.3}\text{Sn}_{0.7}\text{O}_{3-\delta}$  cells, respectively at 520 °C. Besides, the polarization resistance reduced significantly and promote the higher activity of the electrode [20]. All the fitted parameters obtained from the Zsimpwin software have been listed in Table 1 and 2. The lower value of ohmic resistance ( $R_o$ ), as well as grain boundary resistance ( $R_1$ ), signify better conduction of  $\text{SrCo}_{0.3}\text{Sn}_{0.7}\text{O}_{3-\delta}$  - $\text{CeO}_2$  as compared to the  $\text{SrCo}_{0.3}\text{Sn}_{0.7}\text{O}_{3-\delta}$  at 420–520 °C.

To understand the charge transfer phenomenon and ionic conduction process in semiconductor heterostructure  $\text{SrCo}_{0.3}\text{Sn}_{0.7}\text{O}_{3-\delta}$  - $\text{CeO}_2$  cell, different gases environments were applied to observe the changes in the impedance curve as presented in Fig. 5(a and b). Fig. 5(a) shows the impedance curve the fuel cell under the environment of air on both sides of the cell operated at 520 °C. As displayed, several depressed arcs showed much high resistance of about  $40\text{--}50 \Omega\text{-cm}^{-2}$ , signifying that ionic

**Table 1 – The EIS fitted data of the  $\text{SrCo}_{0.3}\text{Sn}_{0.7}\text{O}_{3-\delta}$  - $\text{CeO}_2$  buffer layer electrolyte cell materials at different temperatures 520–420 °C.**

T	L	$R_o$	$R_1$	$Q_1$	n	$R_2$	$Q_2$	n
520 °C	2.997E-8	0.16	0.06	0.004	0.8	0.25	0.0003	0.18
470 °C	1.049E-7	0.21	0.08	0.99	0.4	0.36	0.0004	1
420 °C	1.322E-7	0.26	0.1	0.0002	1	1.19	0.57	0.44

**Table 2 – The EIS fitted data of the  $\text{SrCo}_{0.3}\text{Sn}_{0.7}\text{O}_{3-\delta}$  electrolyte cell materials at different temperatures 520–420 °C.**

T	L	$R_o$	$R_1$	$Q_1$	n	$R_2$	$Q_2$	n
520 °C	7.07E-8	0.25	0.07	2.9	0.79	0.418	3.52	0.24
470 °C	7.464E-8	0.27	0.22	4.02	0.84	0.81	0.75	0.4
420 °C	7.479E-8	0.69	0.41	1.13	0.37	1	0.17	0.1

conduction is negligible. Afterward,  $\text{H}_2$  gas was injected to replace air for 10–15 min, and it resulted in the low ohmic resistance  $0.17 \Omega\text{-cm}^{-2}$ , as well as lower polarization resistance  $0.31 \Omega\text{-cm}^{-2}$ , which is significantly lower than that air/air condition at 520 °C as shown in Fig. 5(b).

Moreover, at first, the  $\text{H}_2$  was replaced with  $\text{N}_2$  and air for almost 1 h. Afterward, the  $\text{N}_2$  was replaced with air to create an air atmosphere on both sides of the cell. Surprisingly, it showed virtually approaching impedance value to the impedance value of the cell under  $\text{H}_2/\text{air}$  condition. These results suggest that ohmic resistance does not change much, while the polarization resistance did not repeat the same value as observed before the performance. This indicates that dominant conduction is the ionic conduction, especially oxygen ions, and proton ions are the charge carrier. Such high ionic conduction is also due to the incorporation of a pure layer of ceria ( $\text{CeO}_2$ ) into the  $(\text{SrCo}_{0.3}\text{Sn}_{0.7}\text{O}_{3-\delta})$  layer to form the heterostructure [43].

#### UV-visible, UPS, and energy band analysis

To further confirm the above proposed mechanism of energy band structure, including the energy levels of  $\text{SrCo}_{0.3}\text{Sn}_{0.7}\text{O}_{3-\delta}$  and  $\text{CeO}_2$ . Therefore, UV-vis and UPS were employed to determine the energy band structure of  $\text{SrCo}_{0.3}\text{Sn}_{0.7}\text{O}_{3-\delta}$  and  $\text{CeO}_2$  separately. Fig. 6(a–b) shows the UV-vis absorption spectra of both semiconductors, both p-type ( $\text{SrCo}_{0.3}\text{Sn}_{0.7}\text{O}_{3-\delta}$ ) and n-type ( $\text{CeO}_2$ ). The energy bandgap is calculated from the precise absorption edges by using the following equation  $\alpha h\nu = A(h\nu - E_g)^n$  in which  $h\nu$  is photon energy  $\alpha$  is the coefficient used for absorption, A represents the constant while n is  $\frac{1}{2}$  value for direct bandgap-semiconductor [44]. The obtained bandgap values 2.11 eV and 3.21 eV for the  $\text{SrCo}_{0.3}\text{Sn}_{0.7}\text{O}_{3-\delta}$  and  $\text{CeO}_2$ , respectively.

However, the bandgap study is not going to fulfill the requirements of the energy level of semiconductors. Therefore, for a better understanding of the energy level, the UPS was performed to determine the position of the valence band using the following equation  $\phi = 21.2 \text{ eV} - (E_{\text{cut-off}} - E_{\text{on-set}})$  [44]. The details of the above-stated equation can be found elsewhere [44]. According to the above-stated equation related to UPS, the position of VB was found to be 6.02 eV and 7.15 eV for the  $\text{SrCo}_{0.3}\text{Sn}_{0.7}\text{O}_{3-\delta}$  and  $\text{CeO}_2$ , respectively. Consequently, the extracted CB position was 3.91 and 3.94 eV by deducting the value of bandgap from the valence band.

The above-determined parameters indicate that  $\text{SrCo}_{0.3}\text{Sn}_{0.7}\text{O}_{3-\delta}$  p-type and  $\text{CeO}_2$  n-type are complementary and suitable to form the p-n heterojunction. Also, by seeing the conduction type of these two p and n-type semiconductor materials, we assume that a successful demonstration occurred due to the formation of p-n heterojunction at particle scale. In p-n heterojunction, charges distribution took place at the interface of either p-type  $\text{SrCo}_{0.3}\text{Sn}_{0.7}\text{O}_{3-\delta}$  or n-type  $\text{CeO}_2$  material, which caused to induce the gradient energy level as well as built-in electric field at the interface. Both phenomena are beneficial in the separation of the ions and electrons, preventing the short-circuiting issue and simultaneously enhancing the fuel cell performance as reported in the published literature [41,45,46]. The interfacial redistribution of charges establishes a space charge region or depletion region, including BIEF, directed from n-type to p-type semiconductor [47]. Also, p-type and n-type materials have different Fermi levels, so to reach a continuous level, valence band offset and conduction band offset were produced to form the potential barrier at particle scale. However, the established potential barrier helps in the stopping of the intrinsic electronic transport. In the meantime, at the interface, built-in electrostatic potential caused to enhance the ionic conduction leads to lower activation energy  $E_{\text{act}}$  [23,40,41,48]. This p-n heterojunction at particle scale level supports the high OCV and the remarkable performance of the fuel cell.

#### Durability of fuel cell

The stability with good and long-term performance is essential in fulfilling the need for the commercialization of semiconductor ionic fuel cell device and technology. Thus, to

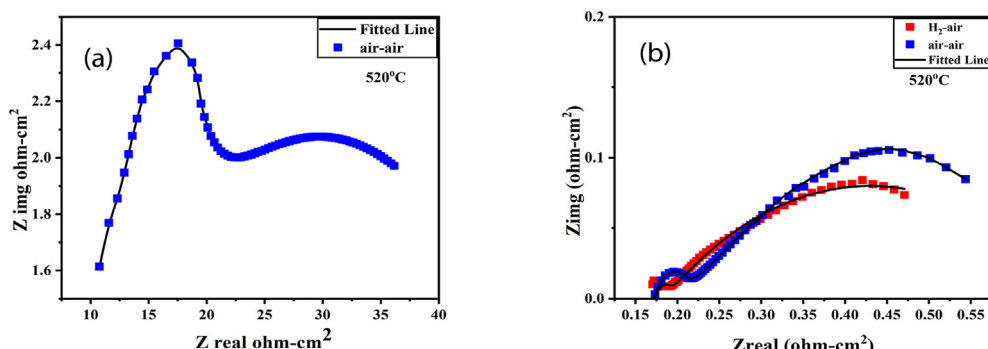


**Fig. 5 – Impedance Spectra of the bi-layer cell operated at 520 °C with (a) air/air and (b)  $\text{H}_2/\text{air}$  then air/air at 520 °C.**

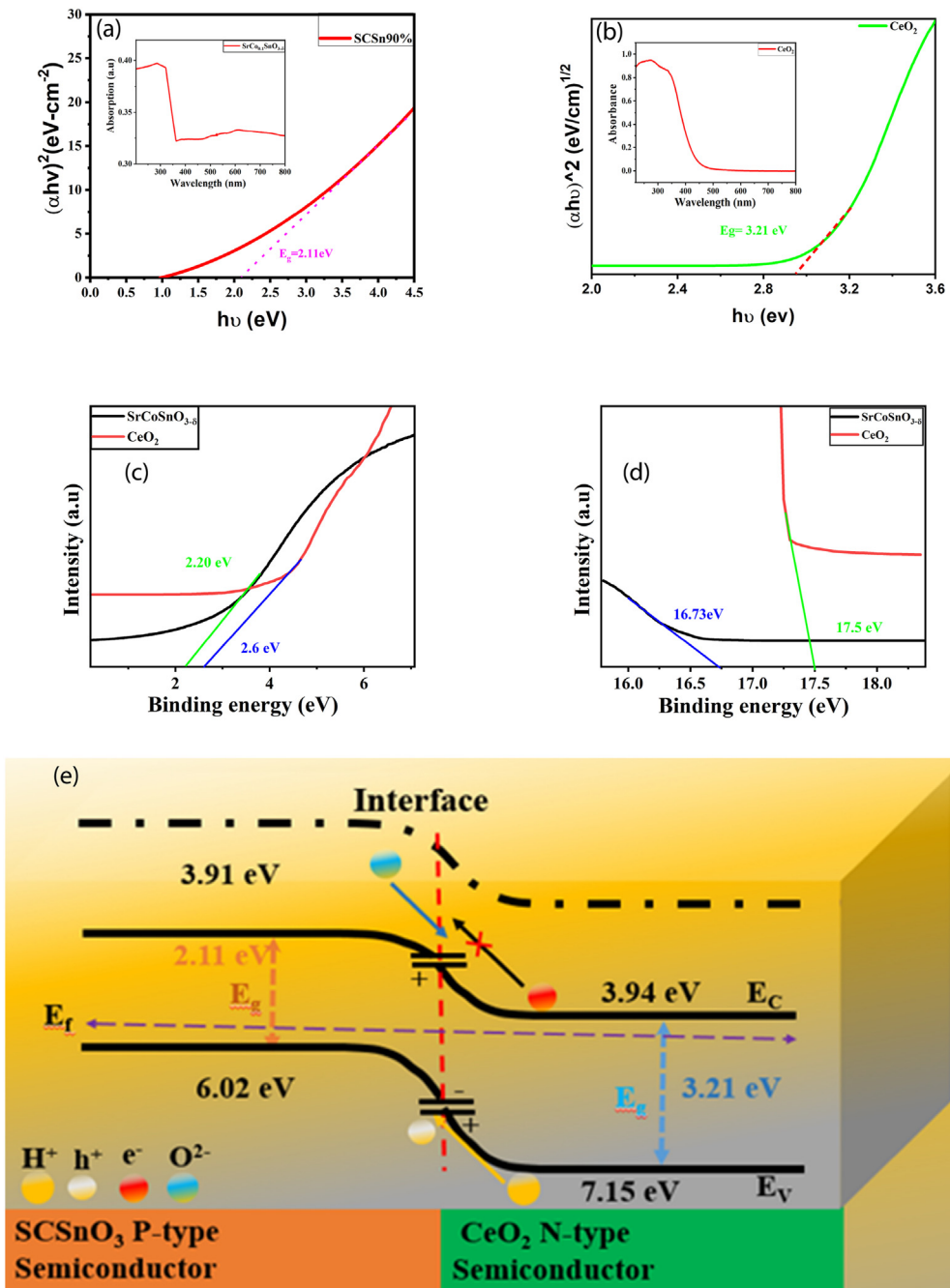


**Fig. 6 – (a–b)** Uv-visible spectra, **(c–d)** UPS spectra and **(e)** band diagram of  $\text{SrCo}_{0.3}\text{Sn}_{0.7}\text{O}_{3-\delta}$  and  $\text{CeO}_2$ .

confirm the feasibility and stability operation of our device including either the single layer (Ni/NCAL-SrCoSnO<sub>3</sub>-NCAL/Ni) or bilayer device (Ni/NCAL/SrCoSnO<sub>3</sub>-CeO<sub>2</sub>/NCAL/Ni) were evaluated under the H<sub>2</sub>/air atmosphere at low operational temperature 520 °C. In our evaluated device the constant current density under the load of 100 mA/cm<sup>2</sup> were applied and noted the stability operation where single layer remain stable at 0.93 V for almost 12 h while the bi-layer hold the stable operation at 0.94 V for 50 h as displayed in Fig. 7. At

start there is little decline in voltage which might be due to the fluctuation in fuel supplying but later it got stable as can be viewed in Fig. 7. From the stability operation It can be concluded that bilayer device is more stable than the single layer which might be appears due to the formation of heterojunction between p and n-type materials.

The long-term stability is necessary for the commercialization of semiconductor based ceramic fuel cell. But keep in mind that long term stability (>100 h) desire a better

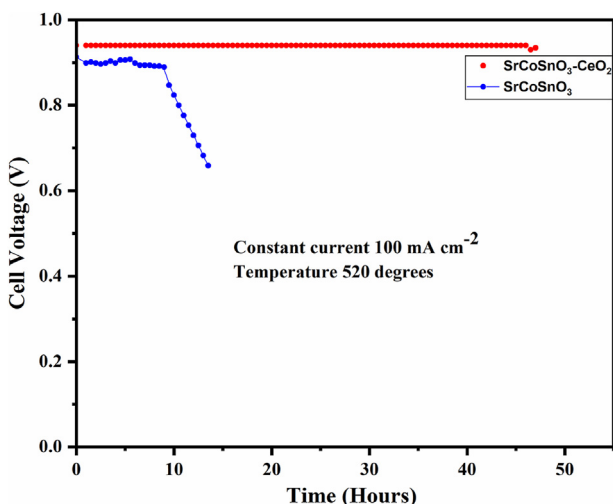


**Fig. 7 – Durability test of single  $\text{SrCoSnO}_3$  layer and bilayer  $\text{SrCoSnO}_3\text{-CeO}_2$  electrolyte under  $\text{H}_2/\text{Air}$  environment at 520 °C.**

engineering in terms of high and stable electrocatalytic activity electrodes and better compatibility which can be persuaded in near future for both either the single layer or bilayer device.

## Conclusion

In summary, we have developed the  $\text{SrCo}_{0.3}\text{Sn}_{0.7}\text{O}_{3-\delta}$  and  $\text{CeO}_2$  as a bi-layer electrolyte for ceramic fuel cells. This study shows that the electrochemical performance of the cells strongly depends on the formation of the heterojunction with the built-in electric field at the interface of n ( $\text{CeO}_2$ ) and p ( $\text{SrCo}_{0.3}\text{Sn}_{0.7}\text{O}_{3-\delta}$ ) semiconductor. The BIEF promotes the transportation of ions to enhance the performance of the device. The bi-layer electrolyte improves the ionic conductivity by 50% as compared to  $\text{SrCo}_{0.3}\text{Sn}_{0.7}\text{O}_{3-\delta}$  based single layer electrolyte. Furthermore, the cells utilizing this bi-layer electrolyte produced 672 mW/cm<sup>2</sup>, whereas the cells utilizing  $\text{SrCo}_{0.3}\text{Sn}_{0.7}\text{O}_{3-\delta}$  single layer electrolyte produced 360 mW/cm<sup>2</sup>. The formation of heterojunction in the bi-layer electrolyte blocks electronic transport through the cell. It hence prevents the short-circuiting as well as enhance the overall performance of the device. Furthermore, our device remains stable almost for 50 h which enlarge the worth of semiconductor device. All these properties and enhanced electrochemical performance of bi-layer semiconductor electrolyte have proven the worth of it to be used in semiconductor based ceramic fuel cell. Thus, semiconductor electrolyte has provided new and vast functionalities to design novel semiconductor electrolyte for advanced ceramic fuel cell technology.

## Declaration of competing interest

The authors declare that they have no known competing financial interests or personal relationships that could have appeared to influence the work reported in this paper.

## Acknowledgment

This work was supported Southeast University (SEU) PROJET # 3203002003A1 and National Natural Science Foundation of China (NSFC) under the grant # 51772080 and 11604088. Dr. Asghar thanks the Hubei overseas Talent 100 program (as a distinguished professor at Hubei University) and Academy of Finland (Grant No. 13329016, 13322738) for their support.

## REFERENCES

- [1] Badwal S. Zirconia-based solid electrolytes: microstructure, stability and ionic conductivity. *Solid State Ionics* 1992;52:23–32.
- [2] Shitara K, Moriasa T, Sumitani A, Seko A, Hayashi H, Koyama Y, et al. First-principles selection of solute elements for Er-stabilized  $\text{Bi}_2\text{O}_3$  oxide-ion conductor with improved long-term stability at moderate temperatures. *Chem Mater* 2017;29:3763–8.
- [3] Sanna S, Esposito V, Andreasen JW, Hjelm J, Zhang W, Kasama T, et al. Enhancement of the chemical stability in confined  $\delta\text{-Bi}_2\text{O}_3$ . *Nat Mater* 2015;14:500–4.
- [4] Gao Z, Mogni LV, Miller EC, Railsback JG, Barnett SAJE, Science E. A perspective on low-temperature solid oxide fuel cells. *Energy Environ Sci* 2016;9:1602–44.
- [5] Chen G, Sun W, Luo Y, He Y, Zhang X, Zhu B, et al. Advanced fuel cell based on new nanocrystalline structure  $\text{Gd}_{0.1}\text{Ce}_{0.9}\text{O}_2$  electrolyte. *ACS Appl Mater Interfaces* 2019;11:10642–50.
- [6] Skinner SJ, Kilner J. Oxygen ion conductors. *Science* 2003;6:30–7.
- [7] Shao Z, Haile SM. A high-performance cathode for the next generation of solid-oxide fuel cells. *Materials for sustainable energy: a collection of peer-reviewed research and review articles from nature publishing group: world scientific. Mater. Sustainable Energy Appl.* 2011:255–8.
- [8] Ralph J, Schoeler A, Krumpelt M. Materials for lower temperature solid oxide fuel cells. *J Mater Sci* 2001;36:1161–72.
- [9] Bellino MG, Sacanell JG, Lamas DG, Leyva AG, Walsöe de Reca N. High-performance solid-oxide fuel cell cathodes based on cobaltite nanotubes. *J Am Chem Soc* 2007;129:3066–7.
- [10] Dong D, Yao J, Wu Y, Zhang X, Xu G, Li C-Z, et al. A 3D fibrous cathode with high interconnectivity for solid oxide fuel cells. *Electrochim Commun* 2011;13:1038–41.
- [11] Shao L, Wang Q, Fan L, Wang P, Zhang N, Sun KJCC. Copper cobalt spinel as a high performance cathode for intermediate temperature solid oxide fuel cells. *Chem Commun (J Chem Soc Sect D)* 2016;52:8615–8.
- [12] Sun J, Liu X, Han F, Zhu L, Bi H, Wang H, et al.  $\text{NdBa}_{1-x}\text{Co}_{2}\text{O}_{5+\delta}$  as cathode materials for IT-SOFC. *Solid State Ionics* 2016;288:54–60.
- [13] Kim J-H, Manthiram A.  $\text{LnBaCo}_2\text{O}_{5+\delta}$  oxides as cathodes for intermediate-temperature solid oxide fuel cells. *J Electrochim Soc* 2008;155:B385–90.
- [14] Zhao E, Ma C, Yang W, Xiong Y, Li J, Sun C. Electrospinning  $\text{La}_{0.8}\text{Sr}_{0.2}\text{Co}_{0.2}\text{Fe}_{0.8}\text{O}_{3-\delta}$  tubes impregnated with  $\text{Ce}_{0.8}\text{Gd}_{0.2}\text{O}_{1.9}$  nanoparticles for an intermediate temperature solid oxide fuel cell cathode. *Int J Hydrogen Energy* 2013;38:6821–9.
- [15] Chen Y, Nie X, Wang B, Xia C, Dong W, Wang X, et al. Tuning  $\text{La}_{0.6}\text{Sr}_{0.4}\text{Co}_{0.2}\text{Fe}_{0.8}\text{O}_{3-\delta}$  perovskite cathode as functional electrolytes for advanced low-temperature SOFCs. *Catal Today* 2019;355:295–303.

- [16] Garcés D, Soldati AL, Troiani H, Montenegro-Hernández A, Caneiro A, Mogni LV. La/Ba-based cobaltites as IT-SOFC cathodes: a discussion about the effect of crystal structure and microstructure on the O<sub>2</sub>-reduction reaction. *Electrochim Acta* 2016;215:637–46.
- [17] Chen G, Sun W, Luo Y, Liu H, Geng S, Yu K, et al. Investigation of layered Ni<sub>0.8</sub>Co<sub>0.15</sub>Al<sub>0.05</sub>LiO<sub>2</sub> in electrode for low-temperature solid oxide fuel cells. *Int J Hydrogen Energy* 2018;43:417–25.
- [18] Wang B, Cai Y, Xia C, Liu Y, Muhammad A, Wang H, et al. CoFeZrAl-oxide based composite for advanced solid oxide fuel cells. *Electrochim Commun* 2016;73:15–9.
- [19] Xia C, Wang B, Ma Y, Cai Y, Afzal M, Liu Y, et al. Industrial-grade rare-earth and perovskite oxide for high-performance electrolyte layer-free fuel cell. *J Power Sources* 2016;307:270–9.
- [20] Fan L, Su P-C. Layer-structured LiNi<sub>0.8</sub>Co<sub>0.2</sub>O<sub>2</sub>: a new triple (H<sup>+</sup>/O<sup>2-</sup>/e<sup>-</sup>) conducting cathode for low temperature proton conducting solid oxide fuel cells. *J Power Sources* 2016;306:369–77.
- [21] Garcia-Barriocanal J, Rivera-Calzada A, Varela M, Sefrioui Z, Iborra E, Leon C, et al. Colossal ionic conductivity at interfaces of epitaxial ZrO<sub>2</sub>: Y<sub>2</sub>O<sub>3</sub>/SrTiO<sub>3</sub> heterostructures. *Science* 2008;321:676–80.
- [22] Lee S, Zhang W, Khatkhatay F, Wang H, Jia Q, MacManus-Driscoll JL. Ionic conductivity increased by two orders of magnitude in micrometer-thick vertical yttria-stabilized ZrO<sub>2</sub> nanocomposite films. *Nano Lett* 2015;15(11):7362–9.
- [23] Mushtaq N, Xia C, Dong W, Wang B, Raza R, Ali A, et al. Tuning the energy band structure at interfaces of the SrFe<sub>0.75</sub>Ti<sub>0.25</sub>O<sub>3-δ</sub>–Sm<sub>0.25</sub>Ce<sub>0.75</sub>O<sub>2-δ</sub> heterostructure for fast ionic transport. *ACS Appl Mater Interfaces* 2019;11(42):38737–45.
- [24] Lin Y, Fang S, Su D, Brinkman KS, Chen F. Enhancing grain boundary ionic conductivity in mixed ionic–electronic conductors. *Nat Commun* 2015;6:6824.
- [25] Zu F, Amsalem P, Ralaifarisoa M, Schultz T, Schlesinger R, Koch N. Surface state density determines the energy level alignment at hybrid perovskite/electron acceptors interfaces. *ACS Appl Mater Interfaces* 2017;9(47):41546–52.
- [26] Zhu B, Lund PD, Raza R, Ma Y, Fan L, Afzal M, Patakangas J, He Y, Zhao Y, Tan W, Huang QA. Schottky junction effect on high performance fuel cells based on nanocomposite materials. *Advanced Energy Materials* 2015;5(8):1401895.
- [27] Fan L, Ma Y, Wang X, Singh M, Zhu B. Understanding the electrochemical mechanism of the core–shell ceria–LiZnO nanocomposite in a low temperature solid oxide fuel cell. *J Mater Chem* 2014;2(15):5399–407.
- [28] Zhu B, Lund P, Raza R, Patakangas J, Huang QA, Fan L, Singh M. A new energy conversion technology based on nano-redox and nano-device processes. *Nanomater Energy* 2013;2(6):1179–85.
- [29] Wu Y, Zhu B, Huang M, Liu L, Shi Q, Akbar M, Chen C, Wei J, Li JF, Zheng LR, Kim JS. Proton transport enabled by a field-induced metallic state in a semiconductor heterostructure. *Science* 2020;369(6500):184–8.
- [30] Rauf S, Zhu B, Shah MK, Tayyab Z, Attique S, Ali N, Mushtaq N, Wang B, Yang C, Asghar MI, Lund PD. Application of a triple-conducting heterostructure electrolyte of Ba<sub>0.5</sub>Sr<sub>0.5</sub>Co<sub>0.1</sub>Fe<sub>0.7</sub>Zr<sub>0.1</sub>Y<sub>0.1</sub>O<sub>3-δ</sub> and Ca<sub>0.04</sub>Ce<sub>0.80</sub>Sm<sub>0.16</sub>O<sub>2-δ</sub> for high performance low-temperature solid oxide fuel cell. *ACS Appl Mater Interfaces* 2020;12(31):35071–80.
- [31] Rauf S, Shah MY, Ali N, Mushtaq N, Tayyab Z, Yousaf M, Yang CP, Wang B. Tuning semiconductor LaFe<sub>0.65</sub>Ti<sub>0.35</sub>O<sub>3-δ</sub> to fast ionic transport for advanced ceramics fuel cells. *Int J Hydrogen Energy* 2020;46(15):9861–73.
- [32] Wang B, Zhu B, Yun S, Zhang W, Xia C, Afzal M, et al. Fast ionic conduction in semiconductor CeO<sub>2-δ</sub> electrolyte fuel cells. *NPG Asia Mater* 2019;11:1–12.
- [33] Xing Y, Wu Y, Li L, Shi Q, Shi J, Yun S, et al. Proton shuttles in CeO<sub>2</sub>/CeO<sub>2-δ</sub> core-shell structure. *ACS Energy Lett* 2019;4(11):2601–7.
- [34] Shah MY, Mushtaq N, Rauf S, Akbar N, Xing Y, Wu Y, et al. Advanced fuel cell based on semiconductor perovskite La–BaZrYO<sub>3-δ</sub> as an electrolyte material operating at low temperature 550° C. *Int J Hydrogen Energy* 2020;45:27501–9.
- [35] Shah MY, Rauf S, Mushtaq N, Zhu B, Tayyab Z, Yousaf M, et al. Novel perovskite semiconductor based on Co/Fe-codoped LBZY (La<sub>0.5</sub>Ba<sub>0.5</sub>Co<sub>0.2</sub>Fe<sub>0.2</sub>Zr<sub>0.3</sub>Y<sub>0.3</sub>O<sub>3-δ</sub>) as an electrolyte in ceramic fuel cells 2021.
- [36] Rauf S, Zhu B, Shah MY, Xia C, Tayyab Z, Ali N, et al. Tailoring triple charge conduction in BaCo<sub>0.2</sub>Fe<sub>0.1</sub>Ce<sub>0.2</sub>Tm<sub>0.1</sub>Zr<sub>0.3</sub>Y<sub>0.1</sub>O<sub>3-δ</sub> semiconductor electrolyte for boosting solid oxide fuel cell performance. *Renew Energy* 2021;172:336–49.
- [37] Mushtaq N, Lu Y, Xia C, Dong W, Wang B, Shah MY, et al. Promoted electrocatalytic activity and ionic transport simultaneously in dual functional Ba<sub>0.5</sub>Sr<sub>0.5</sub>Fe<sub>0.8</sub>Sb<sub>0.2</sub>O<sub>3-δ</sub>–Sm<sub>0.2</sub>Ce<sub>0.8</sub>O<sub>2-δ</sub> heterostructure. *Appl Catal B Environ* 2021;120:503.
- [38] Wang S-F, Hsu Y-F, Yeh C-T, Huang C-C, Lu H CJSS. Characteristics of SrCo<sub>1-x</sub>Sn<sub>x</sub>O<sub>3-δ</sub> cathode materials for use in solid oxide fuel cells. *Solid State Ionics* 2012;227:10–6.
- [39] Shah MY, Rauf S, Mushtaq N, Tayyab Z, Ali N, Yousaf M, Xing Y, Akbar M, Lund PD, Yang GP, Zhu B. Semiconductor Fe-doped SrTiO<sub>3-δ</sub> perovskite electrolyte for low-temperature solid oxide fuel cell (LT-SOFC) operating below 520 °C. *Int J Hydrogen Energy* 2020;45(28):14470–9.
- [40] Shah MAKY, Mushtaq N, Rauf S, Xia C, Zhu B. The semiconductor SrFe<sub>0.2</sub>Ti<sub>0.8</sub>O<sub>3-δ</sub>–ZnO heterostructure electrolyte fuel cells. *Int J Hydrogen Energy* 2019;44:30319–27.
- [41] Xia C, Mi Y, Wang B, Lin B, Chen G, Zhu B. Shaping triple-conducting semiconductor BaCo<sub>0.4</sub>Fe<sub>0.4</sub>Zr<sub>0.1</sub>Y<sub>0.1</sub>O<sub>3-δ</sub> into an electrolyte for low-temperature solid oxide fuel cells. *Nat Commun* 2019;10:1707.
- [42] Fan L, Wang C, Chen M, Zhu B. Recent development of ceria-based (nano) composite materials for low temperature ceramic fuel cells and electrolyte-free fuel cells. *J Power Sources* 2013;234:154–74.
- [43] Chen G, Liu H, He Y, Zhang L, Asghar MI, Geng S, et al. Electrochemical mechanisms of an advanced low-temperature fuel cell with a SrTiO<sub>3</sub> electrolyte. *J Mater Chem A* 2019;7:9638–45.
- [44] Dong W, Tong Y, Zhu B, Xiao H, Wei L, Huang C, et al. Semiconductor TiO<sub>2</sub> thin film as an electrolyte for fuel cells. *J Mater Chem A* 2019;7:16728–34.
- [45] Wang H, Zhang L, Chen Z, Hu J, Li S, Wang Z, et al. Semiconductor heterojunction photocatalysts: design, construction, and photocatalytic performances. *Chem Soc Rev* 2014;43:5234–44.
- [46] Lund PD, Zhu B, Li Y, Yun S, Nasibulin AG, Raza R, et al. Standardized procedures important for improving single-component ceramic fuel cell technology. *ACS Energy Letter* 2017;2:2752–5.
- [47] Li C, Dong S, Tang R, Ge X, Zhang Z, Wang C, et al. Heteroatomic interface engineering in MOF-derived carbon heterostructures with built-in electric-field effects for high performance Al-ion batteries. *Energy Environmenatl Sciences* 2018;11:3201–11.
- [48] Baliga B. Power semiconductor devices (general engineering). PWS Pub. Co; 1995.